2010-01-01

PK/PD Modelling of Comb-Shaped PEGylated Salmon Calcitonin Conjugates of Differing Molecular Weights

Sinead Ryan
Dublin Institute of Technology, sinead.ryan@dit.ie

Jesus Maria Frias
Dublin Institute of Technology, Jesus.Frias@dit.ie

David H. Haddleton
University of Warwick

David J. Brayden
University College Dublin, david.brayden@ucd.ie

Recommended Citation

Brayden, D J. et al. (2010) PK/PD modelling of comb-shaped PEGylated salmon calcitonin conjugates of differing molecular weights. *Journal of Controlled Release.* 149(2) 126-132. doi:0.1016/j.jconrel.2010.10.004

PK/PD modelling of combed-shaped PEGylated salmon calcitonin conjugates of differing molecular weights

Sinéad M. Ryan [a,b], Jesús M. Frías [b], David M. Haddleton [c]

and David J. Brayden [a,*]

[a] UCD School of Veterinary Medicine and UCD Conway Institute, University College Dublin, Belfield, Dublin 4, Ireland; [b] School of Food Science and Environmental Health, Dublin Institute of Technology, Cathal Brugha Street, Dublin 1, Ireland; [c] Department of Chemistry, University of Warwick, Coventry CV4 7AL, UK

* Corresponding author. Tel.: +353 1 7166013; fax: +353 1 7166019.

E-mail address: david.brayden@ucd.ie

Abstract

Salmon calcitonin (sCT) was conjugated via cysteine-1 to novel combed-shaped end-functionalised poly(PEG) methyl ether methacrylate) (sCT-P) comb-shaped polymers, to yield conjugates of total molecular weights (MW) inclusive of sCT: 6.5, 9.5, 23 and 40 kDa. The conjugates were characterised by HPLC and their *in vitro* and *in vivo* bioactivity was measured by cAMP assay on human T47D cells and following intravenous (i.v.) injection to rats, respectively. Stability against endopeptidases, rat serum and liver homogenates was assessed. There were linear and exponential relationships between conjugate MW with potency and efficacy respectively, however the largest MW conjugate still retained 70% of E_{max} and and an EC50 of 3.7 nM. *In vivo*, while free sCT and the conjugates reduced serum [calcium] to a maximum of 20-30 % in 240 min, the half life (T½) was increased and area under the curve (AUC) was extended in proportion to conjugate MW. Likewise, the polymer conferred protection on sCT against attack by trypsin, chymotrypsin, elastase, rat serum and liver homogenates, with the best protection afforded by sCT-P (40 kDa). Mathematical modelling accurately predicted the MW relationships to *in vitro* efficacy, potency, *in vivo* PK and enzymatic stability. With a T½ of 8 hr, the 40 kDa MW comb-shaped PEG conjugate of sCT may have potential as a long-acting injectable formulation.

Keywords: salmon calcitonin, PEGylation, conjugated peptides, osteoporosis, pharmacokinetic modelling, comb-shaped polymers

1. Introduction

Inadequate delivery is a barrier to the effective administration of many promising biotech molecules [1]. Parenterally-administered proteins and peptides tend to be either rapidly cleared from circulation by the reticuloendothelial system or metabolised by serum and liver peptidases leading to loss of biological activity. Oral delivery is even more problematic than the parenteral route, as peptide and protein-based molecules are metabolised by serine proteases, degraded at varying intestinal pH values, and have poor small intestinal epithelial permeability (i.e. typical Class III agents in the Biopharmaceutical Classification System) [2]. A number of strategies have been devised to improve the pharmacokinetics (PK) for parenterally-administered proteins and some small molecules. Otherwise multiple injections are needed, which reduce compliance and efficacy. One of the most successful commercial approaches has been the covalent attachment of poly (ethylene glycol), i.e. PEGylation [3, 4]. The improved PK is largely attributed to the increased molecular size conferred by PEG on the conjugate, thereby masking the protein surface from proteolytic attack, decreasing recognition by phagocytes of the RES, and reducing renal glomerular filtration [5]. Examples of marketed long-acting injected PEGylated biopharmaceuticals are the anti-VEGF aptamer, Pegaptanib (Macugen®, OSI Pharmaceuticals, USA), for treatment of wet macular degeneration, and also Pegfilgrastim (Neulasta®, Amgen Ltd, USA), granulocyte-stimulating colony factor (G-CSF) for treatment of chemotherapy-induced neutropenia.

In this study, sCT was used to further examine a novel type of comb-shaped PEGylation. sCT (molecular weight (MW) 3432 Da) is a 50 times more potent analogue of human CT, a small 32 amino acid peptide secreted by the C cells of thyroid gland [6].

The primary structure of sCT is characterised by a disulfide bridge between two cysteine residues at positions 1 and 7 and a proline amide moiety at the C terminus; it also displays an α-helix and β-sheet, but has no tertiary structure. The main physiological role of CT is control of serum calcium levels in conjunction with parathyroid hormone through actions on the intestine, kidneys and bone. In bone, sCT acts primarily by inhibiting osteoclast cell-mediated bone resorption, although recent studies suggest that it may have an independent anabolic effect on chrondrocytes [7]. It is licenced to treat hypercalcaemia, Paget's disease and as a second-line treatment for post-menopausal osteoporosis. Although its analgesic effects are well known, there is renewed commercial interest in the peptide due to its potential anti-inflammatory actions in osteoarthritis [8]. It is administered by subcutaneous or intra-muscular injections, or more commonly via the nasal route [9]. Due to its short terminal half-life of approximately 60 min following parenteral administration, injections up to twice a day can be required and patient compliance tends to be low. Nasal delivery of calcitonin however, can lead to irritation of the nasal mucosa, blocked sinuses and rhinitis in some subjects [10]. Although preferable to nasal, successful oral formulations of sCT have been elusive and none have yet been marketed [11]. Similarly, longer-acting injections of sCT would have an obvious advantage over the current injected systemic formulations for osteoporosis and may have additional application in local intra-articular delivery for osteoarthritis.

We recently demonstrated specific cysteine-1 conjugation of sCT to a combed-shaped end-functionalised poly(PEG- methyl ether methacrylate) comb-shaped polymer, (sCT-P) [12]. The 6.5 kDa MW conjugate had increased proteolytic stability compared to both free sCT and a linear PEG version of similar total MW. In addition to lengthening

the half-life of sCT following injection to rats, *in vitro* and *in vivo* efficacy and potency was retained by the conjugate compared to free sCT and the linear PEGylated conjugate [12]. The aim of the present study was to evaluate the effects of increasing the MW of the comb-shaped polymer conjugated onto sCT on both *in vitro* bioactivity and *in vivo* PK following i.v. injection to rats. Whilst increased polymer MW generally improves peptide stability and PK parameters, it may interfere with biological functions at the receptor level due to steric hindrance [13]. Therefore, an appropriate polymer size should be selected so as to balance pharmacodynamics (PD) and PK. We therefore synthesized a range of sCT-P conjugates of different molecular weights attached to the methacrylate group via cysteine-1 and investigated *in vitro* biological activity, stability and cytotoxicity. Since PK/PD modelling is an important tool in the design of optimally PEGylated biomolecules, we also assessed PK and PD in rats following i.v. delivery. A two compartment PK model was used to model free sCT kinetics and a first order process was able to model the release of free sCT from the conjugates. We then compared the release rate constants (k_{rel}) between polymers and ascertained the effects of MW. The data show clear relationships between overall conjugate MW, *in vitro* efficacy and the capacity for protection against enzymatic metabolism.

2. Materials and Methods

2.1. *Materials*

sCT was purchased from PolyPeptide Laboratories (Denmark). The Parameter™ cAMP (EIA) kit was obtained from R&D systems, UK, and the sCT (EIA) kit was purchased from Bachem (UK). mPEG aldehyde (M_n = 5.0 kDa) was purchased from Nektar Therapeutics (CA, USA) and $Na(CN)BH_3$ was from Sigma Aldrich, UK. Tissue culture reagents were obtained from BioSciences, Ireland. All other chemicals used were of reagent grade.

2.2. *Synthesis of sCT- poly(poly(ethylene glycol) methyl ether methacrylate) (sCT-P) conjugates*

Poly(poly(ethylene glycol) methyl ether methacrylate) of different molecular weights were prepared by Transition Metal-Mediated Living Radical Polymerization (TMM-LRP) [14, 15]. Each polymer was conjugated to the *N*-terminal cys-1 at of sCT by reductive amination [16]. To make sCT-P (6.5 kDa), a solution of sCT (100 mg, 0.029 mmol) in 100mM acetate buffer pH 5.0 (30 mL) was added to a solution of 6.5 kDa aldehyde-functionalised poly(poly(ethylene glycol) methyl ether methacrylate) (1.91 g, 0.29mmol), previously dissolved in 30 mL of the same buffer. Aqueous 25 mM $NaCNBH_3$ (3.0 mL, 0.075mmol) was then added and the resulting solution was left stirring at ambient temperature and monitored by RP-HPLC, taking 150 μL aliquots of the reaction mixture and dilute them in 1.35 mL of mobile phase A (90 % HPLC grade water, 10 % MeCN and 0.05 % TFA) prior to analysis. The final conjugates were then purified by cationic ion-exchange fast protein liquid chromatography (IE-FPLC) using a

gradient of NaCl in 20 mM aqueous sodium acetate (pH 4.0). The MW of the sCT-P conjugates were: 6.5, 9.5, 23 and 40 kDa, each inclusive of the sCT (3.4 kDa) component.

2.3. *Reverse Phase HPLC analysis*

Characterization of sCT-P conjugates of differing MW was monitored by reverse phase (RP) HPLC. Samples were analyzed with a Varian 920 HPLC using a Luna 5µ C18(2) column 250 × 4.6 mm (Phenomenex, UK). Gradient elution was carried out at a flow rate of 1.0 mL/min, with a mobile phase A containing: 99.9% H_20 and 0.1% tri-fluoroacetic acid (TFA), and a mobile phase B, containing: 99.9% acetonitrile and 0.1% TFA. The gradient sequence was: 20-35% B from 0-10 min, 35-37% B from 10-20 min and 37-20% B from 20-25 min. Samples were monitored at a UV absorbance of 215 nm and 280 nm.

2.4. *MW analysis of sCT-P conjugates*

The sCT-P (6.5 kDa) conjugate were analyzed by matrix assisted laser desorption ionization-time of flight mass spectrometry (MALDI-TOF MS, Bruker UltraFlex III MALDI-TOF mass spectrometer) and size-exclusion chromatography (SEC)-HPLC. SEC-HPLC was carried out on the other conjugates (9.5, 23, 40 kDa) using a BioSep-SEC-S-2000 and S-3000 columns 300 × 7.8 mm (Phenomenex, UK). Samples were eluted with 50 mM PO_4 pH 6.8 at a flow rate of 1 mL/min, and monitored at a UV absorbance of 215 nm and 280 nm. MALDI-TOF MS was not suitable for these

larger MW samples. The integrity and purity of the derivatives were monitored using RP-HPLC (Section 2.3).

2.5. Identification of the PEGylation site of sCT on PolyPEG® derivatives

Identification of the attachment site of poly(poly(ethylene glycol) methyl ether methacrylate) to cys-1 of sCT was confirmed by selective tryptic digestion [17]. Briefly, 50-200 µM of sCT-P was digested using trypsin (0.5 µM) in ammonium bicarbonate buffer (0.05 M) incubated at 37°C for a minimum of 12 hr. The reaction was stopped by addition of 5 % acetic acid. The trypsin-digested samples were analyzed using RP-HPLC and MALDI-TOF MS.

2.6. *In vitro bioactivity: intracellular cAMP stimulation in human T47D cells*

The capacity of sCT-P conjugates to increase intracellular cAMP was assessed in by an established method [18]. Briefly, T47D human breast cancer cells expressing calcitonin receptors were maintained in RPMI-1640 culture medium containing 1 % penicillin–streptomycin, 10 % fetal bovine serum, and insulin (0.2 IU/mL). Cells were seeded on 24 well plates at an initial density of 1.0×10^6 cells/well and incubated in 95% air and 5% CO_2 at 37 °C for 24 hr. Media was replaced with serum-free media and incubated for a further 24 hr. After washing with HBSS, cells were pre-incubated with the serum free medium supplemented with the phosphodiesterase inhibitor 3-isobutyl-1-methyl-xanthine (IBMX, 0.2mM) at 37 °C for 30 min. The cells were then incubated with sCT-P conjugates for 15 min. The adenylate cyclase activator, forskolin (10 µM), was used as a positive control. After removing the media, the intracellular cAMP was

extracted from the cells by cell lysis and measured by ELISA. Results were analyzed using the R Statistical Language [19] and represented as an E-max model.

2.7. Stability studies: intestinal enzyme metabolism

sCT-P conjugates were incubated with intestinal enzymes in sodium acetate (50 mM) transport buffer at a pH 4.5. It also contained TPCK (N-p-tosyl-Lphenylalanine chloromethyl ketone)-treated trypsin (0.5 μM), TLCK (1-chloro-3-tosylamido-7-amino-2-heptanone)-treated chymotrypsin (0.1 μM) and elastase (0.48 μM). Enzymes and substrates were incubated separately at 37 °C for 15 min, before co-incubation. Samples were withdrawn at 0, 1, 5, 10, 15, 20, 30 and 60 min. All samples were analyzed both for the capacity to induce cAMP in T47D cells and for structural stability by RP-HPLC [12]. Rate constants and half lives for sCT-P conjugates were calculated by assuming first order kinetics.

2.8. ***Stability studies: rat liver homogenates and serum***

A fresh liver (7.5 g), harvested from a euthanized Wistar female rat (240 g) was soaked in ice cold saline and homogenized in 10mM PBS at pH 7.4. The mixture was centrifuged at 2000 rpm at 4°C for 2 min, and the supernatant was collected. Rat serum was collected by centrifugation (8500 rpm, 15 min) at 4°C. Protein concentrations were measured and adjusted to the final bovine serum albumen (BSA) equivalent concentration of 20mg in 10mM PBS (pH 7.4). After 15 min equilibration at 37°C, liver homogenates or serum were then co-incubated with sCT-P conjugates. Samples were taken at 0, 1, 5,

10, 15, 20, 30 and 60 min when the reaction was stopped. All samples were analyzed for bioactivity on T47D cells.

2.9. *Lactate dehydrogenase (LDH) release and transepithelial electrical resistance (TEER) measurements in Caco-2 monolayers*

Caco-2 cells were cultured as filter-grown monolayers according to previous methods [20]. At confluence, Caco-2 cells were seeded at a density 5×10^5 cells/well on polycarbonate Transwell® inserts (Costar catalogue # 3401) and grown in a humidified 37°C incubator with 5 % CO_2 in air. Adequate barrier formation of monolayers was tested by measuring the TEER of monolayers before experiments using an EndOhm® electrode system (World Precision Instruments, UK) with background correction made for unseeded filters. Monolayers were rinsed with phenol-red-free HEPES-buffered-DMEM medium and allowed to equilibrate at 37°C for 60 min. sCT and sCT-P conjugates were added to the apical side of monolayers at a concentration of 1 μM. Medium and SDS (0.1 %) were used negative and positive controls respectively. Samples were taken from the apical side at different time points for 120 min and assayed for LDH release using an ELISA microplate reader (Tecan SpectraFlour Plus®). The absorbance was measured at 450 nm, with the reference absorbance at 620 nm. Cell viability was expressed as the percentage of absorbance of test compounds compared with that of cells incubated with media alone. TEER across confluent monolayers was assessed as an additional surrogate of cytotoxicity in the presence and absence of polymers [20].

2.10. ***Hypocalcaemia and PK of sCT-P conjugates in rats***

7-8 week-old male Wistar rats (200-300g) were anesthetized using intra-peritoneal injections of ketamine (75 mg/kg) and xylazine (10mg/kg). Rats were injected *via* the tail vein at a dose of 40µg/kg (i.e. 200 IU/mL/kg) sCT for each formulation in triplicate unless stated. 0.2mL blood samples were obtained via cardiac puncture using a 26G needle fitted with a 1mL heparinised syringe before administration and then typically at 15, 30, 60, 120, 180, 240, 360 and 480 min after injection. Serum samples were analyzed for calcium using a Randox Laboratory clinical chemistry colorimetric analyzer at a wavelength of 612 nm [12]. sCT concentrations in serum were detected by using an EIA kit (Bachem, UK), with a limit of detection of 0.02-25ng/mg. PK parameters including AUC and terminal T½ were calculated using WinNonLin® 5.2 software (Pharsight Corp., USA). All animal experimental procedures in the study adhered to the Principles of the Laboratory Animal Care (NIH Publication# 85–23, revised in 1985) and were performed in compliance with the Irish Department of Health and Children animal licence number, B100/3709, following approval by the University College Dublin Animal Research Ethics Sub-committee.

2.11. ***Two compartmental model analysis of sCT in vivo data***

A two compartmental model considering serum (central) and peripheral pools (Fig. 1A) was used to describe the PK of serum sCT following i.v. injection to rats [21, 22]. Considering first order for sCT movement, the resulting system of ordinary differential equations (ODE) defining the Model I were:

$$dy_1/dt = -k_{12}\, y_1 + k_{21}\, y_2 - k_{deg}\, y_1 \qquad \text{(Eq.1)}$$

$dy_2/dt = k_{12} y_1 + k_{21} y_2$ (Eq. 2)

Where k_{12} and k_{21} are the first rate transfer constants between compartment 1 and 2 and vice versa, and k_{deg} is the first order degradation constant of sCT in serum [21]. To these three unknown parameters, the sCT_0, the initial concentration resulting from the i.v injection in the serum compartment (y_1 @ t=0) was added to accommodate for intra-subject variation. The initial concentration of sCT in the inner compartment was assumed to be zero. Non-linear least squares regression was used to calculate the parameters k_{12}, k_{21}, k_{deg} and sCT_0 (sCT in central compartment at time of i.v. injection).

2.12. Two compartmental model analysis of sCT-polymer derivatives in vivo data

To further model the PK of the sCT-P conjugates, a first order release process of sCT from the conjugates to release free sCT to the central compartment was added to Model I to yield Model II (Fig. 1B). Assuming first order for all transfers, the system of ODE defining Model II is:

$dy_1/dt = -k_{12} y_1 + k_{21} y_2 - k_{deg} y_1 + k_{rel} y_3$ (Eq.3)

$dy_2/dt = k_{12} y_1 - k_{21} y_2$ (Eq.4)

$dy_3/dt = -k_{rel} y_3$ (Eq. 5)

Where k_{12} and k_{21} are the first rate transfer constants between compartment 1 and 2 and vice versa, k_{deg} is the first order degradation constant of free sCT in serum as described in Model I, and k_{rel} is the first order release constant of sCT from the polymer. To those 4

unknown parameters, $y_{3,0}$ the concentration of conjugated sCT after i.v. injection in the polymer compartment 3 (y_3 @ t=0) needs to be estimated with possibly a random effect to allow for variations in dose levels between subjects. While k_{rel} may vary between different polymers it could be assumed that the rest of the parameters ($y_{3,0}$, k_{12}, k_{21} and k_{deg}) in the model are shared by free salmon calcitonin and any conjugated polymer of salmon calcitonin. The estimated parameters from Model I were used in Model II to describe the pharmacokinetics of those conjugates while k_{rel} and y_3 was estimated for each conjugated polymer in order to compare the release constants (k_{rel}) between the polymers.

2.13. Statistical analysis

Non-linear regression and nonlinear mixed effect modeling of the ODE models, t-tests, Tukey-HSD post hoc ANOVA comparison and generation of confidence intervals was performed using R Statistical Language [19]. $P < 0.05$ was the required level to denote statistical significance. When using non-linear regression or non-linear mixed-effects modeling, the natural logarithm transformation of the parameters was estimated [21].

3. Results

3.1. Characterization of sCT-P conjugates

Chemical structure, preparation, purification and characterisation of the sCT-conjugated polymers has been previously published extensively by our group, including ion-exchange (IE), reverse-phase HPLC and MALDI-TOF [22, 23]. SEC-HPLC analysis confirmed high purity and predicted the molecular weights of all sCT-P comb-shaped conjugates (Table 1). Conjugation reactions were monitored over time by RP-HPLC where the profile showed a reciprocal relationship between the sCT peak gradually disappearing at an approximate elution volume of 17.0 mL and the conjugate peak gradually appearing over the same period at an approximate elution volume of 20 mL. Fig.2 shows the data for sCT-P (9.5 kDa). sCT-P conjugates were further purified by IE-FPLC, an example shown for the 6.5 kDa conjugate (Fig.3). Fractions obtained from (IE)-FPLC were then analyzed by SEC-HPLC to evaluate purity (Fig.4, 6.5 kDa conjugate). Identification of the attachment site was achieved by analogy as previously described [12]. The conjugation site of the purified conjugates was determined and confirmed by tryptic digestion followed by RP-HPLC and MALDI-TOF MS analysis of the digested fragments (data not shown, but see [12] for data on the sCT-P (6.5 kDa) conjugate).

The intracellular cAMP-generating capacity of the sCT-P conjugates in T47D cells were compared to that free sCT. Free sCT and sCT-P conjugates elevated intracellular cAMP in a concentration-dependent manner (Fig. 5a). The EC_{50} and E_{max} values (Table 2) determined for each conjugate were inserted into a global fit model. From it, an exponential relationship was obtained for the former (Fig. 5b) and a linear relationship was obtained for the latter with respect to MW (Fig. 5c). In sum, the higher

the MW of polymer attached to sCT, the higher the potency and the lower the efficacy. However, even for the largest MW (sCT-P (40 kDa) conjugate, 72 % of E_{max} was still retained compared to free sCT and the potency was within 1-2 log concentrations.

3.3. Stability of sCT-P conjugates: intestinal enzymes, liver homogenates and serum.

The stability of sCT conjugates against exposure to specific intestinal enzymes was analysed by cAMP responses generated in T47D cells. sCT was rapidly degraded within minutes by trypsin, chymotrypsin, elastase and in combination. sCT-P conjugates displayed significantly increased resistance to the individual intestinal enzymes and in combination, and the higher the MW, the greater the protection (Fig. 6). The largest conjugate sCT-P (40 kDa) gave excellent protection to sCT when incubated for 60 min with the three individual enzymes alone and in combination. The degradation half life of sCT-P (40 kDa) was 11 times longer than that of sCT-P (6.5 kDa) ($p<0.005$), when all three proteolytic enzymes were present. An almost identical pattern was also observed for the conjugates in rat liver homogenates and serum (Fig.7). sCT and its conjugates were a little more susceptible to enzymes present in the liver compared to the combination of serine proteases from the small intestine. A comparison of the apparent first order reaction rate constants of each conjugate in the presence of serine proteases, rat blood serum and rat liver homogenate as determined by cAMP measurements on T47D cells revealed that there was a dependence of reaction rate constant (k) of sCT with different MW values of polymer (Fig. 7), and it was confirmed that as the MW of the conjugate increased, the degradation rate of sCT decreased.

3.4. Cytotoxicity evaluations

Cytotoxicity of sCT-P conjugates was assessed on Caco-2 monolayers by LDH assay. sCT conjugates at a concentration of 10 μM showed relatively low levels of cytotoxicity following 120 min exposure (Fig.8). Cytotoxicity increased as the MW of conjugate was increased. For sCT-P (6.5 kDa), just 10% of cells were unviable, whereas for sCT-P (40 kDa), 28% were unviable. The integrity of monolayers exposed to conjugates was also measured by TEER. Similar to the pattern observed for LDH release, the TEER decreased as the MW of the conjugates increased. A maximum TEER decrease of 28% was also observed for sCT-P (40 kDa) compared to Caco-2 exposed to media alone after 120 min. This decrease was reversible upon replacement with drug-free media (data not shown).

3.5. *In vivo* hypocalcaemia and PK of sCT-P conjugates in rats

sCT and sCT-P conjugates were assessed for their capacity to induce a hypocalcaemic response in rats following i.v. injection. At sCT equivalent doses of 200 IU/kg, all sCT–P conjugates reduced plasma [calcium] at 240 min. Compared to free sCT, the calcium profiles after i.v. injections of all sCT conjugates did not show any differences between each other (Table 2). All values were compared to the saline-treated controls over the same period, where no changes in serum [calcium] were detected. Within the first 4 hours, all sCT-P conjugates were equally bioactive. The range of serum [calcium] reduction was 15-30%, and 30% is typically the maximum reduction we detect [12].

Using the same blood samples, [sCT] in plasma were also determined by ELISA following i.v. administration of sCT and sCT-P conjugates. Free [sCT] was rapidly eliminated from the circulation with a $T_{1/2}$ of 41.8 ± 12.4 min (Table 2). In contrast, the sCT-P conjugates demonstrated a much slower elimination rate with a $T_{1/2}$ values of 632, 668 and 1426 min for conjugates 6.5, 23 and 40 kDa respectively. The $T_{1/2}$ values for the sCT-P (6.5 kDa) and sCT-P (23 kDa) were not statistically different due to high inter-animal variations, but their $AUC_{0\text{-}480\ min}$ values were significantly higher than that of free sCT ($P < 0.0001$, $P < 0.05$, respectively). Following the administration of sCT-P (40 kDa), plasma [sCT] was relatively constant, suggesting a sustained release of sCT into the blood (Fig. 9). There was therefore a significantly longer $T_{1/2}$ (1425.6 ± 257.0 min) and larger AUC (16703 ± 9491 ng.min/mL) at 8 hours for the sCT-P (40 kDa) conjugate compared to sCT and the other conjugates.

3.6. PK modelling of sCT following i.v. administration to rats

The plasma concentration of sCT and sCT-P conjugates after i.v. administration was fitted using Model I (free sCT) and Model II (different sCT-P conjugates).
Model I (Fig.1A) predicted the distribution of [sCT] adequately (Fig.10). There was no major variation between subjects that might have affected the process and no introduction of a random effect was necessary. Non-linear regression was used to calculate the kinetic parameters, k_{12}, k_{21} and k_{deg} (Fig.10). The estimated model parameters had an associated error of the order of 10%, which was considered a reasonable precision to predict the fate of free sCT in plasma.

The PK parameters estimated using Model I and free sCT were then used in Model II (Fig.1A) to predict the PK of sCT-P after i.v. injection. In order to complete the model, estimates of the release constant (k_{rel}) and the equivalent initial [sCT] in plasma after injection ($y_{3,0}$) of each individual sCT-P conjugate were built using non-linear mixed effect modelling. On top of those two fixed parameters, and in order to account for the high inter-subject variability observed in the study, a random effect allowing for inter-subject variation in the initial concentration of sCT-P was made. While ($y_{3,0}$) and its corresponding random effect are nuisance parameters that depend on the particular study, k_{rel} provides the generation rate of sCT from sCT-P conjugates, the parameter of interest assuming a controlled release of sCT in serum after i.v. injection is desired. A plot of the natural logarithm of the release rate constant of sCT from the polymer is presented. As the conjugated polymer increased in MW, k_{rel} decreased (Fig.11), providing a longer release period for sCT, which was in agreement with the actual data obtained (Fig 5) CHECK right fig . By fitting the data of all polymers to a single model containing a dependence of the $\ln(k_{rel})$ with the polymer MW, an intercept of -5.4±0.3 $\ln(min^{-1})$ and a slope of -0.053±0.016 $\ln(min^{-1})$ / kD were estimated, confirming a significant effect of MW on the release constant. This suggests that sCT-P (40 kDa) might potentially be a good candidate for a long-lasting depot injection.

4. Discussion

Many technologies and strategies have been developed focusing on improvement of characteristics of protein and peptide drugs to gain the desired PK properties used to extend the half-life of therapeutics, thus enabling much less frequent administration. Some of the technologies include amino acid manipulation to reduce immunogenicity and proteolytic instability, genetic fusion to immunoglobulins domains or serum proteins (albumin) and post-production modifications and conjugation with natural or synthetic polymers. PEGylation, is a well-established, widely used, fast growing technology that has an excellent track record in the formulation of safe and efficacious drug products [3]. It is considered one of the most successful techniques in that injected PEGylated therapeutics are currently used for the treatment of many diseases [25, 26]. Polymer conjugation can also confer targeting properties to reach disease sites including tumors [27- 29]. Several efficacious and safe PEGylated products have been on the market for over 15 years, and ten PEGylated products have been approved to date [30].

Although PEG is an approved biocompatible polymer, individual components of the methacrylate-based PEG, (poly(poly(ethylene glycol) methyl ether methacrylate) are neither. Important components include the methacrylic backbone and the terminal aldehyde, and they have previously shown to induce low cytotoxicity to Caco-2 and mucous-covered HT29-MTX-E12 intestinal monolayers [12]. While increasing MW of the polymer seemed to increase cytotoxicity in Caco- 2 using the LDH and TEER read-outs, levels were still low. Studies will need to be carried out to examine the fate of poly(poly(ethylene glycol) methyl ether methacrylate) and its metabolites in body compartments and tissues once the MW is increased, as there is potential for

accumulation. This is especially relevant in the current example where the polymer is the major component of the conjugate compared to the peptide, and where repeated dosing will be necessary. The kidney clearance threshold of protein is estimated at 60 kDa [4]. Assuming that polymer hydrodynamic volume will almost double the effective molecular diameter, similar to branched PEGs [31], sCT-P (40 kDa) will therefore be too large for kidney filtration if it is not ultimately metabolized into smaller components. In theory, the PEG teeth should break away from the methacrylate backbone due to esterase action, thereby permitting renal filtration and this is the basis of ongoing study. It is notable that while PEG itself has Generally Regarded As Safe (GRAS) status as a "non-active" excipient, there are historical reports that it can induce epithelial vacuolisation in rat renal cortical tubules following chronic repeated parenteral administration of high doses of large MW PEGs [32]. Bolon et al. [33] also showed that increasing the length of a 20kDa PEG chain, converting it to a branched format or adding extra PEG molecules reduced renal vacuolization in mice. Most evidence however would support the view that PEG has such a history of safe use that its conjugation to peptides should not pose any particular concern [34], aside perhaps from the relatively unexamined potential for immunotoxicology induction following administration in high doses. An initial toxicology study carried out in rats using a commercially available form of the comb-shaped polymer (PolyPEG®, Warwick Effect Polymers, UK), did not find any evidence of vacuolisation in renal epithelia following repeated dosing of up to 200mg to rats [35]. While clearly undesirable, there is little evidence to date however that vacuolisation has any deleterious effects on renal function.

The main drawback associated with peptide and protein PEGylation is the potential for reduced biological activity, however, this can be compensated by a longer elimination T½ and reduced clearance. A well-cited example is PEGylated interferon α-2a (Pegasys®, Roche, USA). The 40 kDa branched PEG conjugate retained only 7% of the antiviral activity of the native protein, still displayed improved PK following weekly injections *in vivo* in hepatitis C patients [36, 37]. In contrast, bioactivity analysis from the T47D cAMP assay indicated that the potency and efficacy of sCT-P of increasing MW compared well to native sCT, with sCT-P (40 kDa) retaining 72% of the maximum bioactivity. From the global fit model, a linear and indirect relationship was established between efficacy and conjugate MW and there was an exponential and direct dependence on EC_{50} with conjugate MW. It appears therefore that access to the CT receptor has not been impeded by conjugation to cysteine-1 and there is no evidence that sCT simply dissociates from the polymer in solution [12]. This bioassay is a useful tool to estimate efficacy and potency of any polymer conjugated to cAMP-inducing peptides.

sCT has multiple peptidase cleavage sites and is therefore susceptible to proteolytic degradation in the small intestine. To reduce metabolism, a linear lys-18-PEG_{2K}-sCT displayed enzymatic stability, reduced systemic clearance and enhanced hypocalcaemia following intra-duodenal administration to rats [38]. Another sCT-mPEG conjugate with mono- and di- mixtures also had reduced clearance and an extended $T_{1/2}$ compared to unmodified sCT [39]. For the sCT-Lys_{18}-PEG conjugates, increased proteolytic stability and an extended $T_{1/2}$ are clearly associated with increased PEG MW [40]. sCT-P (6.5 kDa) conjugated to cys-1 was more stable than native sCT and, more importantly, than sCT conjugated to linear sCT-PEG (5 kDa) [12]. All sCT comb-shaped

conjugates showed substantial resistance to the individual serine proteases, trypsin, chymotrypsin and elastase alone and in combination, as well as following exposure to rat serum and liver homogenates. Improved stability was observed as the MW of the conjugate increased, with sCT-P (40 kDa) providing almost total protection. In our assessment of stability, we used *in vitro* bioactivity analysis as a PD surrogate, since we previously showed a very close correlation between the cAMP assay and HPLC analysis, with the functional read-out being more sensitive [12].

Serum [calcium] and [sCT] following i.v. administration of sCT were measured. Free sCT and the sCT conjugates induced similar hypocalcaemia and the reductions obtained were typical of the maximum achieved following either i.v. administration to rats [41] or s.c. administration to mice [42]. The non-linear relationship between calcium reduction and sCT concentration indicates a highly complex relationship [22, 43], and there is obvious difficulty in screening formulation efficacy when the window of the reduction is so narrow. Thus, sCT-induced hypocalcaemia may not be as sensitive as measurements of plasma [sCT] and its associated PK. Still, all sCT conjugates were bioactive *in vivo*, thus confirming data the *in vitro* bioassay. Serum [sCT] decreased rapidly following i.v. administration of free sCT and levels were below the detection limit after 120 min. The conjugates were, however, detectable up to 8 hr following administration and sCT-P (40 kDa) yielded a T½ over 30 times longer than sCT. For interferon-α 2a, plasma concentrations did not peak until 23-26 hr following i.v. administration of a PEGylated conjugate of similar MW (43 kDa) as the sCT-P (40 kDa) conjugate [44]. It seems that the peak concentration of sCT may occur later than 8 hr

following administration of sCT-P (40 kDa), and it may therefore be a good candidate as a long lasting depot injection.

Recently, models of the PK/PD relationship for sCT have described the interactions between osteoclasts and osteoblasts [45, 46]. One model was related to changes in cellular activities, while other models investigated the mechanism of the effects of sCT and parathyroid hormone. Compartmental models have been previously used to describe the kinetics of sCT [22], and the present work confirms that the PK of free sCT can be well characterized with a two-compartmental model after i.v. injection. Free sCT quickly disappears from serum and the kinetics allow simple predictive modelling of its removal by degradation. From this, we further modelled release of sCT from conjugates, assuming a first order release mechanism. Simple equations allowed estimation of the parameter of physiological relevance in releasing sCT from sCT-P,(i.e. k_{rel}), and allowed comparison between the different MW conjugates. The decrease in k_{rel} in the presence of comb-shaped polymers of increasing MW was statistically significant and the data indicated that manipulation of MW within ranges that are acceptable from manufacturing, efficacy and toxicological standpoints will permit formulations that can extend the T½. A sensitivity of the release rate constant k_{rel} to differences in MW of the conjugated polymer of 0.053±0.016 ln(min^{-1}) reduction per kD was calculated. This parameter quantifies the effect of the conjugated polymer chain length on PK and provides indications on how to design appropriate conjugates for specific applications. One drawback in this strategy is the increased variability in PK between subjects with sCT-P compared to free sCT, and this is especially evident in the case of sCT-P (40kD).

5. Conclusions

A PEG-based combed-shaped methacrylate polymer was conjugated to a specific amino acid of sCT to yield a pure bioactive conjugate, which retained receptor binding capacity. The conjugate was made using and economical and simple process of living radical polymerisation and has been characterised using a range of HPLC techniques, denoting purity and entrapment of most free sCT. By increasing the polymer chain length, a series of conjugates of increasing MW were produced, for which relationships with *in vitro* potency and efficacy were established. The largest MW conjugate (40 kDa) had an extended T½ upon i.v. injection to rats and this more than compensated for the slight losses in potency and efficacy detected *in vitro*. Formulations of such conjugates may have potential for either long-acting systemic injection for osteoporosis or for local intra-articular delivery for treatment of osteoarthritis.

Acknowledgments

This study was funded by Science Foundation Ireland Strategic Research Cluster Grant 07/SRC/B1154. We thank Dr. Clare Sayers at the Chemistry Department, Warwick University, UK, for provision of sCT-P samples. We also thank Dr. Xuexuan Wang of University College Dublin, who carried out the *in vivo* studies.

References

[1] D.K. Malik, S. Baboota, A. Ahuja, S. Hasan, J. Ali, Recent advances in protein and peptide drug delivery systems. Current Drug Delivery 4 (2007) 141-151.

[2] J.H. Hamman, G.M. Enslin, A.F. Kotze, Oral delivery of peptide drugs: barriers and developments. BioDrugs 19 (2005) 165-177.

[3] S.M. Ryan, G. Mantovani, X. Wang, D.M. Haddleton, D.J. Brayden, Advances in PEGylation of important biotech molecules: delivery aspects. Expert Op. Drug Del. 5 (2008) 371-383.

[4] F.M. Veronese, G. Pasut, PEGylation, successful approach to drug delivery. Drug Discovery Today 10 (2005) 1451-1458.

[5] M. Hamidi, A. Azadi, P. Rafiei, Pharmacokinetic consequences of pegylation. Drug Delivery 13 (2006) 399-409.

[6] C. H. Chesnut 3rd, M. Azria, S. Silverman, M. Engelhardt, M. Olson, L. Mindeholm. Salmon calcitonin: a review of current and future therapeutic indications. Osteoporosis. Int. 19 (2008) 479-491.

[7] B-C. Sondergaard, S. H. Madsen, T. Segovia-Silvestre, S. J. Paulsen, T. Christiansen, C. Pedersen, A-C. Bay-Jensen, M. A. Karsdal, Investigation of the direct effects of salmon calcitonin on human chondrocytes, BMC Musculoskeletal Disorders, 11 (2010) 62-71.

[8] M.A. Karsdal, K. Henriksen, M. Arnold, C. Christiansen, Calcitonin: a drug of the past or for the future? Physiologic inhibition of bone resorption while sustaining osteoclast numbers improves bone quality. BioDrugs 22 (2008) 137-144.

[9] H. Hoyer, G. Perera, A. Bernkop-Schnurch, Non-invasive delivery systems for peptides and proteins in osteoporosis therapy: a retro-perspective. Drug Dev. Ind. Pharm. (2009).

[10] P. Peichl, A. Griesmacher, W. Kumpan, R. Schedl, E. Prosquil, H. Bröll H, Clinical outcome of salmon calcitonin nasal spray treatment in postmenopausal women after total hip arthroplasty. Gerontology, 51 (2005) 242-252.

[11] M. A Karsdal, K. Henriksen, A. C. Bay-Jensen, B. Molloy, M. Arnold, , M. R. John, I. Byrjalsen, M. Azria, B. J. Riis, P. Qvist, C Christiansen, Lessons learned from the development of oral calcitonin: the first tablet formulation of a protein in Phase III clinical trials. J. Clin. Pharm. (2010). PMID: 20660294.

[12] S.M. Ryan, X. Wang, G. Mantovani, C.T. Sayers, D.M. Haddleton, D.J. Brayden, Conjugation of salmon calcitonin to a combed-shaped end functionalized poly(poly(ethylene glycol) methyl ether methacrylate) yields a bioactive stable conjugate. J. Control. Release 135 (2009) 51-59.

[13] P. Bailon, C.Y. Won, PEG-modified biopharmaceuticals. Exp. Op. Drug Del. 6 (2009) 1-16.
[14] F. Lecolley, L. Tao, G. Mantovani, I. Durkin, S. Lautru, D.M. Haddleton, A new approach to bioconjugates for proteins and peptides ("pegylation") utilising living radical polymerisation. Chem. Comm. 18 (2004) 2026-2027.
[15] L. Tao, G. Mantovani, F. Lecolley, D.M. Haddleton, Alpha-aldehyde terminally functional methacrylic polymers from living radical polymerization: application in protein conjugation "pegylation". J. Am. Chem. Soc. 126 (2004) 13220-13221.
[16] B. Le Droumaguet, J. Nicolas, Recent advances in the design of bioconjugates from controlled / living radical polymerization. Polymer Chemistry 1 (2010) 563-598.
[17] K.C. Lee, S.C. Moon, M.O. Park, J.T. Lee, D.H. Na, S.D. Yoo, H.S. Lee, P.P. DeLuca, Isolation, characterization, and stability of positional isomers of mono-PEGylated salmon calcitonins. Pharm. Res. 16 (1999) 813-818.
[18] S.B. Fowler, S. Poon, R. Muff, F. Chiti, C.M. Dobson, J. Zurdo, Rational design of aggregation-resistant bioactive peptides: reengineering human calcitonin. PNAS (USA) 102 (2005) 10105-10110.
[19] R. R.D.C. Team, A language and environment for statistical computing, R Foundation for Statistical Computing, Vienna, Austria. http://www.r-project.org. (2008) Accessed May, 2010.
[20] I. Hubatsch, E. G. Ragnarsson, P. Artursson, Determination of drug permeability and prediction of drug absorption in Caco-2 monolayers.Nat. Protoc. 2 (2007) 2111-2119.
[21] D.M. Bates, D.G. Watts, Non-linear regression analysis and its applications, Wiley, New York, (1988).
[22] M. Miyazaki, S. Nakade, K. Iwanaga, K. Morimoto, M. Kakemi, Estimation of bioavailability of salmon calcitonin from the hypocalcemic effect in rats (I): pharmacokinetic-pharmacodynamic modeling based on the endogenous Ca regulatory system. Drug Metabolism and Pharmacokinetics 18 (2003) 350-357.
[23] C. T. Sayers, G. Mantovani, S. M. Ryan, R. K. Randev, O. Keiper, O. I. Leszczyszyn,, C. Blindauer, D. J. Brayden, & D. M. Haddleton (2009), Site-specific N-terminus conjugation of poly($mPEG_{1100}$) methacrylates to salmon calcitonin: synthesis and preliminary biological evaluation, Soft Matter 5 (2009) 3038-3046.
[24] C. T. Sayers. Conjugation of peptides with polymers synthesised via living radical polymerisation. Ph.D. Thesis (2008) University of Warwick, UK.

[25] A. Aghemo, M.G. Rumi, M. Colombo, Pegylated IFN-alpha2a and ribavirin in the treatment of hepatitis C. Exp. Rev. Anti-Infective Therapy, 7 (2009) 925-935.
[26] G. Molineux, Pegfilgrastim: using pegylation technology to improve neutropenia support in cancer patients. Anti-Cancer Drugs 14 (2003) 259-264.
[27] S.J. Denardo, R. Liu, H. Albrecht, A. Natarajan, J.L. Sutcliffe, C. Anderson, L. Peng, R. Ferdani, S.R. Cherry, K.S. Lam, 111In-LLP2A-DOTA polyethylene glycol-targeting α4β1 integrin: comparative pharmacokinetics for imaging and therapy of lymphoid malignancies. J. Nucl. Med. 50 (2009) 625-634.
[28] J.Q. Gao, Y. Eto, Y. Yoshioka, F. Sekiguchi, S. Kurachi, T. Morishige, X. Yao, H. Watanabe, R. Asavatanabodee, F. Sakurai, H. Mizuguchi, Y. Okada, Y. Mukai, Y. Tsutsumi, T. Mayumi, N. Okada, S. Nakagawa, Effective tumor targeted gene transfer using PEGylated adenovirus vector via systemic administration. J. Control. Release 12 (2007) 102-110.
[29] A. Yamada, Y. Taniguchi, K. Kawano, T. Honda, Y. Hattori, Y. Maitani, Design of folate-linked liposomal doxorubicin to its antitumor effect in mice. Clin. Cancer Res. 14 (2008) 8161-8168.
[30] S. Jevsevar, M. Kunstelj, V.G. Porekar, PEGylation of therapeutic proteins. Biotechnol. J. 5 (2010) 113-128.
[31] C. J. Fee, Size comparison between proteins PEGylated with branched and linear poly(ethylene glycol) molecules. Biotechnol. Bioeng. (2007) 725-731.
[32] A. Bendele, J. Seely, C. Richey, G. Sennello, G, Shopp, Short communication: renal tubular vacuolation in animals treated with polyethylene-glycol-conjugated proteins. Toxicol. Sci. 42 (1998)152-157.
[33] B. Bolon, J. Faust, N. Storm, U. Sarmiento, D. Litzinger, O. Kinstler, C. Gegg, M. E. Cozena. Cytoplasmic vacuoles in renal tubular epithelium of mice given polyethylene glycol (PEG)-conjugated proteins are reduced by alternating PEG size and conformation. Toxicologist 60 (2001) 376 [Abstract 1788].
[34] R. Webster, E. Didier, P. Harris, N. Siegel, J. Stadler, L. Tilbury, D. Smith, PEGylated proteins: evaluation of their safety in the absence of definitive metabolism studies. Drug Metab. Dispos. 35 (2007) 9-16.
[35]. S. Walsh, A. Steward, D. M. Haddleton, R. Palmer. Renal epithelial cell vacuolisation induced by cumulative doses of PEG, but not PolyPEG®. PEGS 2008, Boston, MA. http://www.warwickeffectpolymers.co.uk/docs/PolyPEGAbsenceofVacuolisationPosterPEGS2008.pdf. Accessed May, 2010.

[36] P. Bailon, A. Palleroni, C.A. Schaffer, C.L. Spence, W.J. Fung, J.E. Porter, G.K. Ehrlich, W. Pan, Z.X. Xu, M.W. Modi, A. Farid, W. Berthold, M. Graves, Rational design of a potent, long-lasting form of interferon: a 40 kDa branched polyethylene glycol-conjugated interferon alpha-2a for the treatment of hepatitis C. Bioconjug. Chem. 12 (2001) 195-202.
[37] K. Rajender, M.W. Modi, S. Pedder, Use of peginterferon alfa-2a (40 KD) (Pegasys) for the treatment of hepatitis C. Adv. Drug Del. Rev. 54 (2002) 571-586.
[38] Y.S. Youn, J.Y. Jung, S.H. Oh, S.D. Yoo, K.C. Lee, Improved intestinal delivery of salmon calcitonin by Lys18-amine specific PEGylation: stability, permeability, pharmacokinetic behavior and in vivo hypocalcemic efficacy. J. Control. Release 114 (2006) 334-342.
[39] K.C. Lee, K.K. Tak, M.O. Park, J.T. Lee, B.H. Woo, S.D. Yoo, H.S. Lee, P.P. DeLuca, Preparation and characterization of polyethylene-glycol-modified salmon calcitonins. Pharm. Dev. and Tech. 4 (1999) 269-275.
[40]. Y.S. Youn, M.J. Kwon, D.H. Na, S.Y. Chae, S. Lee, K.C. Lee, Improved intrapulmonary delivery of site-specific PEGylated salmon calcitonin: optimization by PEG size selection. J. Control. Release 125 (2008) 68-75.
[41] Y.S. Youn, D.H. Na, K.C. Lee, High-yield production of biologically active mono-PEGylated salmon calcitonin by site-specific PEGylation. J. Control. Release 117 (2007) 371-379.
[42] J. Wang, D. Chow, H. Heiati, W.C. Shen, Reversible lipidization for the oral delivery of salmon calcitonin. J. Control. Release 88 (2003) 369-380.
[43] T. Buclin, J.P. Randin, A.F. Jacquet, M. Azria, M. Attinger, F. Gomez, P. Burckhardt, The effect of rectal and nasal administration of salmon calcitonin in normal subjects. Calcified Tissue Internat. 41 (1987) 252-258.
[44] Y.W. Jo, Y.S. Youn, S.H. Lee, B.M. Kim, S.H. Kang, M. Yoo, E.C. Choi, K.C. Lee, Long-acting interferon-alpha 2a modified with a trimer-structured polyethylene glycol: preparation, in vitro bioactivity, in vivo stability and pharmacokinetics. Int J. Pharm. 309 (2006) 87-93.
[44] S.V. Komarova, R.J. Smith, S.J. Dixon, S.M. Sims, L.M. Wahl, Mathematical model predicts a critical role for osteoclast autocrine regulation in the control of bone remodeling. Bone 33 (2003) 206-215.
[46] V. Lemaire, F.L. Tobin, L.D. Greller, C.R. Cho, L.J. Suva, Modeling the interactions between osteoblast and osteoclast activities in bone remodeling. J. Theoretical Biol. 229 (2004) 293-309.

Figure Legends

Fig. 1. A. Two compartment model of free sCT in rat serum following i.v. administration. B. Two compartmental model describing i.v. PK of sCT-P conjugates.

Fig. 2. RP-HPLC of the conjugation reaction of sCT with P to yield the 9.5 kDa conjugate.

Fig. 3. 6.5 kDa aldehyde functionalised polyPEG conjugated to sCT at a 1:1 ratio, purified using ion-exchange FPLC with online UV detection at 280 nm.

Fig. 4. SEC-HPLC chromatogram of fractions of sCT-$P_{6.5kDa}$ purified by IE-FPLC. The corresponding IE-FPLC chromatogram is also shown for reference (inset).

Fig. 5. Modelling of bioactivity relationship to conjugate MW, determined by cAMP induction in T47D cells. **A**. Concentration-response curves. Continuous lines show prediction of the three parameter dose-response curve fit with hill slope=1. sCT □, sCT-P (6.5 kDa) ◊ , sCT-P (9.5 kDa) ■, sCT-P (23 kDa) ○, sCT-P (40 kDa) ♦. **B.** Relationship of EC_{50} to MW. **C.** Relationship of E_{max} to MW. Discontinuous lines show 95% confidence limits of the prediction.

Fig.6. Degradation profiles of sCT-P conjugates incubated with serine proteases, liver and serum, as determined by cAMP measurement in T47D cells. Curve fitting was based on first order kinetics.

Fig.7. Comparison of degradation rates of the four sCT-P conjugates in the presence of serum, liver homogenates and serine protease enzyme, as determined from cyclic AMP measurements in T47D cells. Mean ± SD of 3 determinations.

Fig.8. LDH release following exposure of Caco-2 monolayers to sCT and sCT-P conjugates (10μM) for 120 min. Mean ± SD of 3 determinations.

Fig.9. sCT levels in rat serum after i.v. administration of sCT (O) and sCT-P (40 kDa) (Δ). Serum samples at time zero in which no sCT was detected were used as the background reading for each animal. Mean ± SD of 3-15 determinations.

Fig.10. Analysis of free sCT data following i.v administration to rats using a two compartmental model to estimate parameters, k_{12},k_{21}, k_{deg} and sCT_0 .

Fig.11. Influence of polymer MW on release rate constant of sCT.

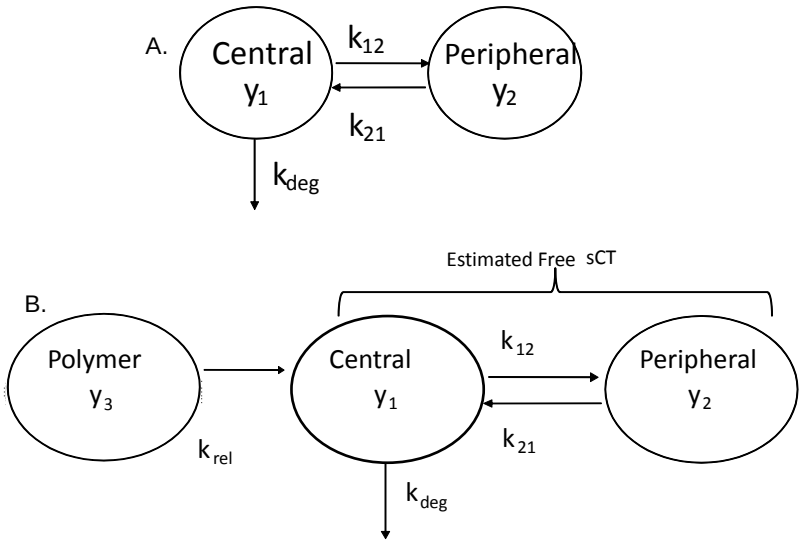

Fig. 1. A. Two compartmental model describing the PK of free sCT in rat serum. B. Two compartmental model describing PK of sCT-P conjugates (i.v.).

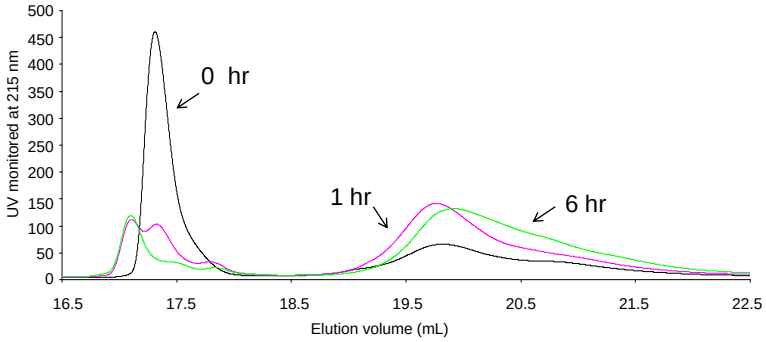

Fig. 2. RP-HPLC spectra following the conjugation reaction of sCT with P to yield a 9.5kDa conjugate.

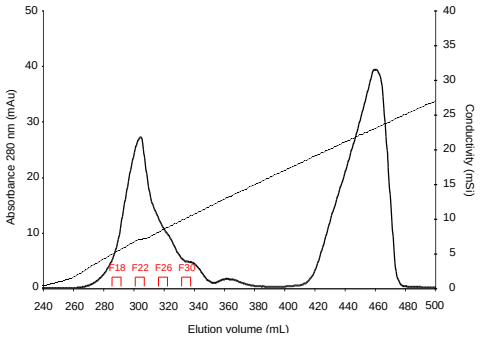

Fig. 3. 6.5 kDa aldehyde functionalised polyPEG conjugated to sCT at a 1:1 ratio, purified using ion-exchange FPLC with online UV detection at 280 nm.

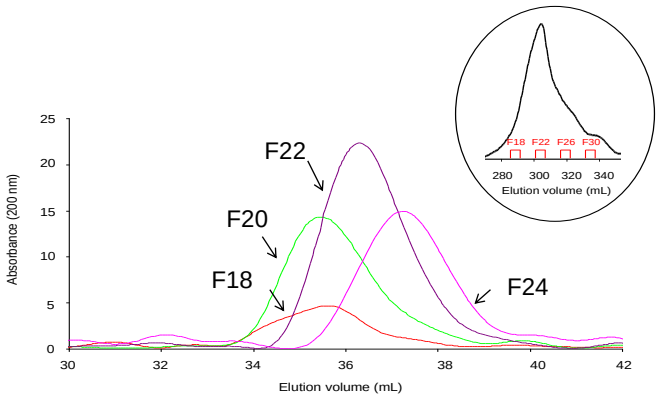

Fig. 4. SEC-HPLC chromatogram of fractions of sCT-$P_{6.5kDa}$ purified by IE-FPLC. The corresponding IE-FPLC chromatogram is also shown for reference (inset).

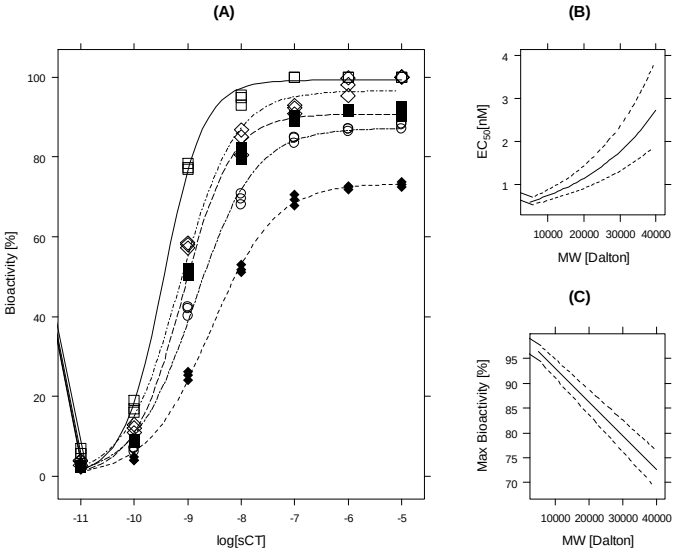

Fig. 5. Modelling of bioactivity relationship to conjugate MW, as determined by cAMP induction in T47D cells. **A**. Concentration-response curves. Continuous lines show prediction of the three parameter concentration-response curve fit with hill slope=1. sCT □, sCT-PEG (5 kDa) ◊ , sCT-P (9.5 kDa) ■, sCT-P (23 kDa) ○, sCT-P (40 kDa) ♦. **B.** Relationship of EC50 to MW. **C.** Relationship of E max to MW. Discontinuous lines show 95% confidence limits of the prediction.

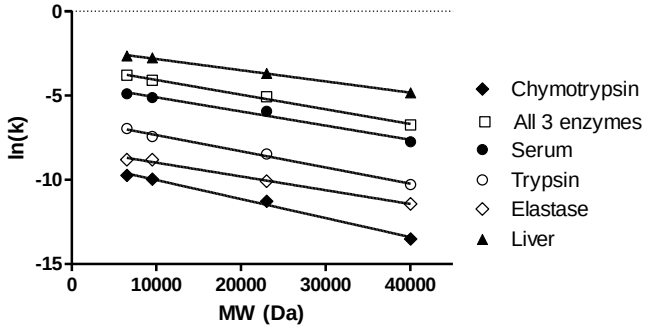

Fig.6. Comparison of degradation rates of sCT-P molecular weight derivatives in the presence of serum and liver and proteases, as determined from cyclic AMP measurements in T47D cells.

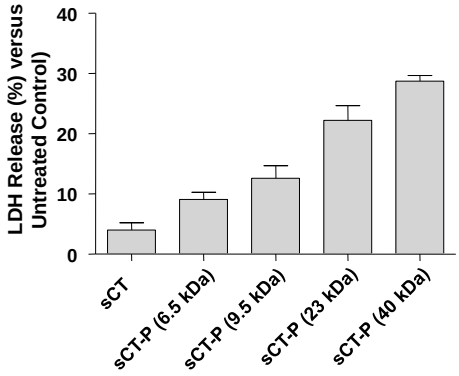

Fig.7. LDH release following exposure of Caco-2 monolayers to sCT and sCT-P conjugates (10 μM) for 120 min. Values were compared to those seen in untreated controls.

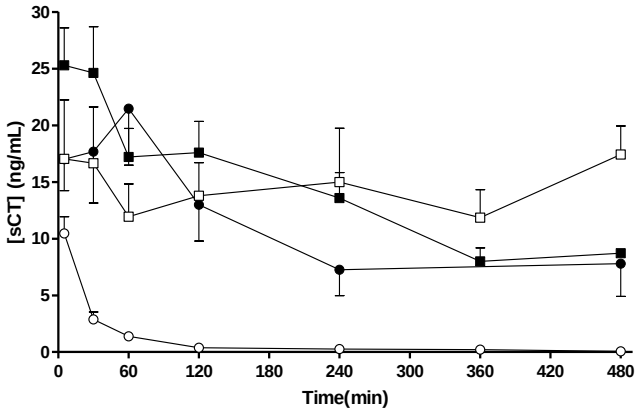

Fig.8. sCT levels in rat serum after i.v. administration of sCT (O), sCT-P (6.5 kDa) ( ), sCT-P (20 kDa) ( ), and sCT-P (40 kDa) ( ). Serum samples at time zero in which no sCT was detected were used as background. Mean SD of 3-15 determinations.

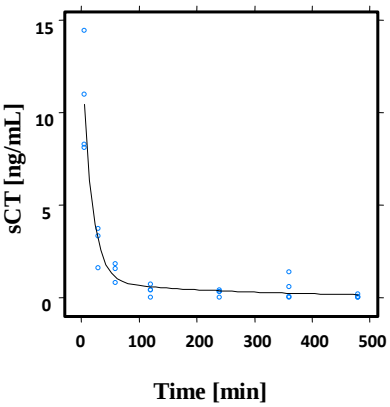

Parameter	Estimate	SEM
k_{12}	0.028 min^{-1}	0.008
k_{21}	0.008 min^{-1}	0.005
k_{deg}	0.026 min^{-1}	0.007
sCT_0	10.44 ng/mL	0.10
σ	0.2 ng/mL	

Fig.9. Analysis of free sCT data following i.v administration to rats using a two compartmental model to estimate parameters, k_{12},k_{21}, k_{deg} and sCT_0 .

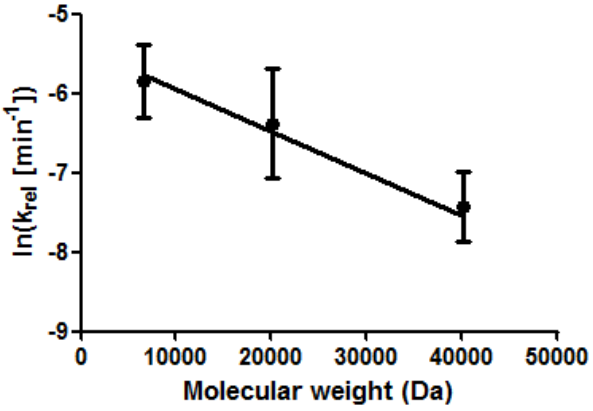

Fig.10. Influence of polymer MW on release rate constant of sCT.